THE JOURNAL OF PHYSICAL CHEMISTRY C

Article

pubs.acs.org/JPCC

Key Role of Ionic Hydrogen Bonding in Nonspecific Protein Adsorption on a Hydrophobic Surface

Nan Li,[†] Junzhu Xiao,[†] Xiaoman Hai,[†] Ke Wang,[†] and Fuquan Dang*[,†,‡]

[†]School of Chemistry and Chemical Engineering and [‡]Key Laboratory of Analytical Chemistry for Life Science of Shaanxi Province, Shaanxi Normal University, 620 West Chang'an Street, Xi'an 710119, China

Supporting Information

ABSTRACT: Nonspecific protein adsorption on the channel walls is a frequently encountered problem in microfluidic chips, resulting in substantial sample loss and low device performance. However, the molecular mechanisms underlying strong interaction of proteins with solid surfaces are largely unknown. Here, we studied the spontaneous adsorption of an ionic complementary peptide EAK16-II [(Ala-Glu-Ala-Glu-Ala-Lys-Ala-Lys)$_2$] and its quaternized derivative QEAK16-II [(Ala-Glu-Ala-Glu-Ala-Lys$_{Me3}$-Ala-Lys$_{Me3}$)$_2$] from solution to a poly(methyl methacrylate) (PMMA) surface. We found that EAK16-II with free ε-amino groups can readily self-organize into a complete coating layer predominantly composed of α-helixes and β-sheets, which efficiently suppress nonspecific adsorption of standard proteins or proteins from human whole blood. Once the free ε-amino groups in EAK16-II are quaternized, QEAK16-II sparsely adsorbs on the PMMA surface with less than 10% coverage, which can be easily substituted by proteins and lead to serious nonspecific protein adsorption similarly to that observed on the pristine PMMA surface. These results clearly indicated the critical role of the ionic hydrogen bonding and eliminate other forces such as hydrophobic, electrostatic, and hydrogen-bonding interactions in the strong adsorption of peptides and proteins on the PMMA surface. Expectedly, the high-performance separations of amino acids, peptides, and proteins were achieved in the PMMA microchannels dynamically coated with EAK16-II and its analogues with different basic amino acid residues in sequence including EAR16-II [(Ala-Glu-Ala-Glu-Ala-Arg-Ala-Arg)$_2$] and EAKR16-II [(Ala-Glu-Ala-Glu-Ala-Arg-Ala-Lys)$_2$]. The present study provides significant insights into the mechanism underlying strong interaction of proteins and peptides with a solid surface.

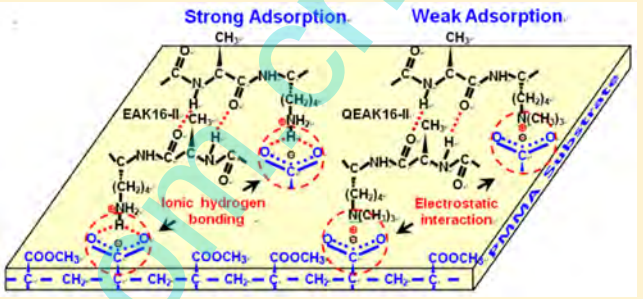

1. INTRODUCTION

Over the past three decades, microfluidic chips have been extensively applied in the fields of chemistry, biology,[1] tissue engineering, biomedicine,[2,3] environmental monitoring,[4] and nanotechnology[5] owing to their intrinsic characteristics of miniaturization, integration, portability, and automation.[6] Various materials such as silicon,[7] glass,[8] poly(methyl methacrylate) (PMMA), polydimethylsiloxane (PDMS),[9] polystyrene (PS), polycarbonate (PC), cyclic olefin copolymers (COC), and poly(vinyl chloride) (PVC)[10] have been applied frequently in fabricating microfluidic chips. Recently, microfluidic chips with various functional elements fabricated in different materials have been extensively explored to perform sophisticated multistep biochemical assays within a single device, allowing for real sample-in−answer-out analysis of complicated biological samples such as whole blood,[3,4,10] saliva,[8] and body fluids.[11−15] Compared with conventional techniques, integrated microfluidic chips can achieve highly sensitive, high-throughput, and low-cost biological and biomedical analyses with small volumes in a short time.[5,10,16−20] However, proteins from complicated biological samples strongly interact with the channel wall of microfluidic chips, leading to surface biofouling and great decrease in device performance.[21−23] Therefore, considerable efforts have been made to develop reliable and reproducible protein-resistant surfaces on various substrate materials, which are basically categorized into physical adsorbed[23−26] and covalent modifications.[27−29] Generally, covalent modifications are laborious multistep processes and case dependent, whereas physical adsorbed methods have limited capabilities in suppressing nonspecific proteins adsorption. The current approaches are not always suitable for integrated microfluidic chips fabricated in different materials. Therefore, a thorough understanding of how proteins interact strongly with a solid surface at the molecular level is necessary to address nonspecific protein adsorption in microfluidic chips.

In nature, spontaneous adsorption of proteins from solution to solid surfaces is fundamental in many natural and industrial processes[30] and has attracted extensive attention in various fields of bionanotechnology,[31] medicine,[32,33] cell biology,[34] pharmaceutical sciences,[35] separation science, enzyme engineering, biomaterials,[36] etc. However, a detailed understanding of

Received: May 23, 2016
Revised: July 16, 2016
Published: August 9, 2016

DOI: 10.1021/acs.jpcc.6b05176
J. Phys. Chem. C 2016, 120, 19135−19141

the molecular mechanisms underlying the strong interaction of proteins with a solid surface is still unrealized.[31−34,37−39] In our previous research,[23] we found that an ionic complementary peptide EAR16-II [(Ala-Glu-Ala-Glu-Ala-Arg-Ala-Arg)$_2$] readily self-organized into a complete monolayer, predominantly composed of tightly packed β-sheets with their hydrophobic and hydrophilic sides exposed to the solution and the surface, respectively, on the native hydrophobic and plasma-oxidized hydrophilic PDMS surfaces. The self-assembled EAR16-II monolayer shows excellent blood compatibility and protein-repelling properties. These results suggested that ionic hydrogen bonding[23,40] between EAR16-II and surface negative charges may play a crucial role in the strong adsorption of peptides and proteins on the PDMS surfaces. To verify our hypothesis, we designed and synthesized an ionic complementary peptide EAK16-II [(Ala-Glu-Ala-Glu-Ala-Lys-Ala-Lys)$_2$] and its quaternized derivative QEAK16-II [(Ala-Glu-Ala-Glu-Ala-Lys$_{Me3}$-Ala-Lys$_{Me3}$)$_2$] and comprehensively investigated their self-assembly on the PMMA surface, a common substrate of microfluidic chips with negative charges in physiological pH condition,[25] using various techniques including microchip electrophoresis (MCE), atomic force microscopy (AFM), water contact angle (WCA), X-ray photoelectron spectroscopy (XPS), attenuated total reflection Fourier transform infrared spectroscopy (ATR-FTIR), and the protein-repelling and blood compatibility measurements. The separations of amino acids, peptides, and proteins were performed in the PMMA microchannels dynamically coated with EAK16-II, EAR16-II, and EAKR16-II [(Ala-Glu-Ala-Glu-Ala-Arg-Ala-Lys)$_2$]. The current work significantly promotes our understanding of nonspecific protein adsorption on a solid surface.

2. EXPERIMENTAL SECTION

Materials and Chemicals. EAK16-II, QEAK16-II, EAR16-II, EAKR16-II, AE16-II [(Glu-Ala-Glu-Ala-Glu-Ala-Glu-Ala)$_2$], and AR16-II [(Ala-Arg-Ala-Arg-Ala-Arg-Ala-Arg)$_2$] (>95% purity by high-pressure liquid chromatography) were synthesized from China Peptides CO., Ltd. (Shanghai, China). Fluorescein isothiocyanate (FITC)−bovine serum albumin (BSA) and FITC−lysozyme (LYZ) were obtained from Zhongkechenyu Corporation (Beijing, China). FITC, arginine (Arg), phenylalanine (Phe), glutamic acid (Glu), glycine (Gly), lysine (Lys), β-lactoglobulin, ribonuclease A, and α-chymotrypsinogen A from bovine pancreas were purchased from Sigma-Aldrich (St. Louis, MO). PMMA sheets were purchased from Nittou Jushi Kogyou Co., Ltd. (Tokyo, Japan). All other chemicals were purchased from local commercial suppliers and were of analytical reagent grade unless otherwise specified. Deionized (DI) water (Milli-Q, Millipore, Bedford, MA) was used to prepare aqueous solutions. All liquid samples were filtered with a 0.22 μm syringe filter to remove particulates before use.

Sample Derivatization. Amino acids (Arg, Phe, Glu, Gly, and Lys), peptides (AE16-II and AR16-II), and proteins (β-lactoglobulin, ribonuclease A, and α-chymotrypsinogen A) were labeled with FITC according to the previous method.[41] Briefly, 10 μL of 0.1 mM amino acids, 1.0 mg/mL peptides, and 1.0 mg/mL proteins in 10 mM phosphate buffer (pH 7.4) were mixed with 10 μL of 10^{-3} M FITC solution in acetone and 80 μL of 20 mM borate buffer (pH 9.4). Then, the mixtures were incubated overnight in the dark at room temperature. Labeled buffer blank samples were also prepared and analyzed for identification of dye hydrolysis products and other impurities. The labeling solutions were stored at −20 °C and used within 2 weeks. The above solutions were diluted to the desired concentrations with running buffer prior to analysis.

Preparation of PMMA Surface Specimens. PMMA slabs (10 mm × 10 mm × 2 mm) were first sonicated in 1.0 M NaOH and DI water for 30 min and dried under vacuum to obtain PMMA substrates. Then, PMMA sheets (1.0 cm × 1.0 cm) were immersed in 1.0 mg/mL EAK16-II and QEAK16-II in 10 mM phosphate buffer (pH 7.4) at 25 °C for 1 h. Afterward, PMMA sheets were pulled out of the solution and dried under 25 °C, then washed copiously with DI water, and dried with N_2. Finally, PMMA specimens were characterized by AFM, WCA, XPS, and ATR-FTIR measurements.

Surface Characterization of PMMA Specimens. The AFM images of the pristine, EAK16-II- and QEAK16-II-modified PMMA surfaces were acquired using a CSPM5500 atomic force microscope (Beijing, China) in tapping mode. The measurements were performed at a scan frequency of 2 Hz using a standard silicon tip with a resonance frequency at 306 kHz. Measurements were made three times on different zones of each PMMA specimen in a scanning area of 2.0 μm × 2.0 μm. WCA measurements were performed using an OCA 20 optical contact angle meter (Dataphysics, Inc., Stuttgart, Germany) via the sessile drop technique using DI water. Each data given was based on ten contact angle measurements at five different positions on PMMA specimens. XPS analyses were performed on an Axis Ultra X-ray photoelectron spectrometer (Kratos Analytical Ltd., Manchester, UK) with an Al X-ray source operating at 150 W (15 kV, 10 mA). The vacuum in the main chamber was kept above 3 × 10^{-9} Pa during XPS data acquisition. The specimens were analyzed at an electron takeoff angle of 45° with respect to the surface plane. General survey scans (binding energy range 0−1200 eV, pass energy 80 eV) and high-resolution spectra (pass energy 75 eV) in the C 1s, O 1s, and N 1s regions were recorded for all modified PMMA substrates. The binding energies (BEs) were referenced to the C 1s binding energy at 284.6 eV. ATR-FTIR was collected using a Tensor 27 infrared spectrometer (Bruker, Billerica, MA) with a wedged germanium crystal of attenuated total reflectance accessory. All spectra of PMMA specimens were obtained at a 45° angle of incidence for 64 scans with a resolution of 4 cm^{-1} in the range of 400−4000 cm^{-1} at room temperature. Circular dichroism (CD) spectra were measured on a Chirascan CD spectrometer (Applied Photophysics Ltd., Leatherhead, UK) ∼20 min after dissolution of EAK16-II and QEAK16-II in 10 mM phosphate buffer (pH 7.4). Spectra were recorded using a 200 μL aliquot of 1.0 mg/mL EAK16-II and QEAK16-II in a 0.1 mm path length quartz cuvette (Hellma) at 25 °C from 260 to 190 nm with 1.0 nm step and 1.0 nm bandwidth. The spectroscopic scans were repeated at least three times and averaged. Background subtraction, molar ellipticity conversion, and data smoothing with a least-squares fit were performed using the Chirascan and CDNN software.[23]

Characterization of Biofouling Resistance and Electrophoresis on Microchannels. Fluorescence microscopy measurements were used to assess nonspecific protein adsorption on microchannels. Protein adsorption assay was performed similarly to the method previously reported.[21,23] Briefly, the pristine as well as EAK16-II- and QEAK16-II-modified PMMA microchannels (100 μm × 40 μm × 30 mm) were filled with 1.0 mg/mL FITC-BSA and FITC-LYZ in 10 mM phosphate buffer (pH 7.4) and incubated at 37 °C for 1 h.

DOI: 10.1021/acs.jpcc.6b05176
J. Phys. Chem. C 2016, 120, 19135−19141

Afterward, protein solution was removed, and the channels were dried under vacuum at 25 °C. After washing with copious DI water and drying under vacuum at 25 °C, the resulting protein contaminated microchannels were imaged using an inverted microscope (Olympus IX51, Tokyo, Japan) with a CCD camera (QIMAGING, Micropublisher 5.0 RTV). Thrombus accumulation and platelet adhesion were performed with in vitro blood flow model.[22,23] The pristine and coated PMMA microchannels were subject to the whole blood, collected from a healthy person containing 3.8 wt % citrate sodium as anticoagulant, and the each experiment process lasted 30 min with 500 μL of human whole blood. Then the microchannels were rinsed with copious 10 mM phosphate buffer (pH 7.4) and dried at 25 °C. The images of PMMA microchannels were recorded with a CCD camera.

MCE of FITC-labeled amino acids, peptides, and proteins were carried out using a laboratory-built system based on an Olympus IX51 inverted fluorescence microscope with a 100 W high-pressure mercury lamp as excitation radiation coupled with a Model N2000 chromatography workstation (Zhejiang University, Hangzhou, China) for data acquisition. Voltages to reservoirs adjustable in the range of −1.5 to +1.5 kV were provided by a HVS448-3000D high voltage sequencer (Lab-Smith, Livermore, CA). PMMA microchip is 85 mm × 50 mm with three simple cross-channels of 100 μm width and 40 μm depth. The distances from the channel crossing point to the sample, sample waste, buffer, and buffer waste reservoirs were 5.25, 5.25, 5.75, and 37.5 mm, respectively. FITC-labeled amino acids, peptides, and proteins were separated at field strength of 270 V/cm in microchannels filled with 20 mM borate buffer (pH 9.4) (pristine channels) or 20 mM borate buffer (pH 9.4) containing 1.0 mg/mL EAK16-II, QEAK16-II, EAR16-II, and EAKR16-II (dynamically coated channels).

Safety Considerations. The MCE used high voltage; hence, special care should be taken when handling the electrophoresis electrodes to avoid possible electrical shock.

3. RESULTS AND DISCUSSION

Characterization of EAK16-II and QEAK16-II Coatings on PMMA Surfaces. It is generally assumed that proteins strongly interact with a solid surface via a collection of various noncovalent interactions such as van der Waals, hydrophobic,[30,31] electrostatic,[32−34] hydrogen bonding,[35,36] and ionic hydrogen bonding interactions.[23] Structurally, EAK16-II interacted with the PMMA surface via the same noncovalent forces as proteins whereas QEAK16-II utilized similar noncovalent forces except for ionic hydrogen bonding. If ionic hydrogen bonding plays a key role in spontaneous adsorption of peptides on the PMMA surfaces, an obvious difference in coating performance of EAK16-II and QEAK16-II on the PMMA channels would be observed. As shown in Figure 1A, the reproducible separation of FITC-Phe and FITC-Arg was obtained in the EAK16-II-coated PMMA channels, whereas no reproducible separation was achieved in the QEAK16-II-modified and pristine PMMA channels due to the strong adsorption of FITC-Arg and FITC-Phe in the channel walls. Based on our previous studies,[25,26] these results indicated that EAK16-II self-organized into a coating layer tightly adsorbed on the PMMA surface and remained intact with copious water or buffer, which greatly suppressed analytes adsorption, whereas QEAK16-II cannot form such an irreversible coating layer on the PMMA surface.

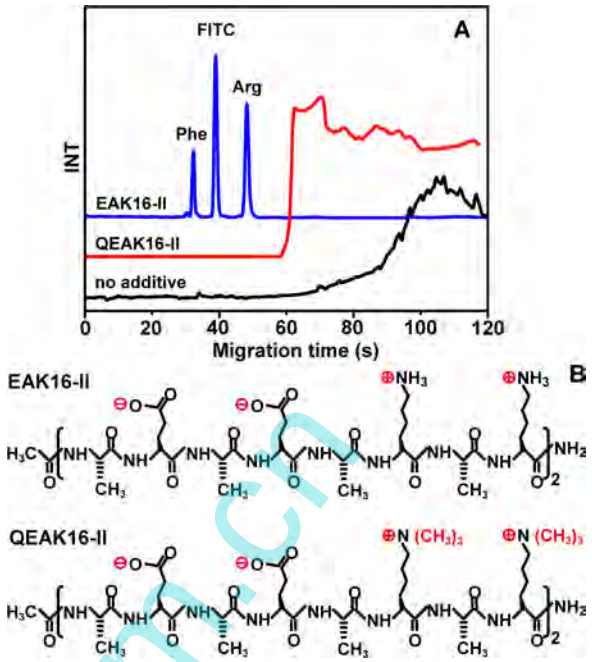

Figure 1. (A) Microchip electropherograms of FITC-labeled Phe and Arg (1.0×10^{-7} M) on the PMMA channels coated with 1.0 mg/mL EAK16-II (blue), 1.0 mg/mL QEAK16-II (red), and the pristine PMMA (black). Conditions: 20 mM borate buffer, pH 9.4, E_{sep} = 270 V/cm, and the effective separation length of 30 mm. (B) Chemical structures of EAK16-II and QEAK16-II.

Next we conducted AFM measurements to confirm whether EAK16-II and QEAK16-II coating layers existed on the PMMA surface. The pristine PMMA exhibits a relatively smooth surface with discernible ridge and valley structures (Figure 2AI). EAK16-II can self-organize into a complete and compact coating layer predominantly composed of tightly packed ribbon-like nanostructures (arrow in Figure 2AII) on the PMMA surface. In contrast, QEAK16-II only shows tiny

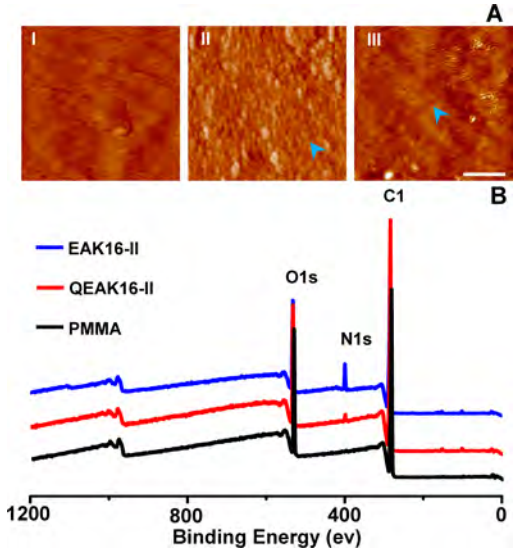

Figure 2. (A) AFM topography images (2.0 μm × 2.0 μm) of the pristine PMMA (I) as well as coated PMMA by EAK16-II (II) and QEAK16-II (III). Scale bar: 500 nm. (B) XPS spectra of the QEAK16-II- and EAK16-II-coated and uncoated PMMA surface.

DOI: 10.1021/acs.jpcc.6b05176
J. Phys. Chem. C 2016, 120, 19135−19141

clusters (arrow in Figure 2AIII) sparsely adsorbed on the surface. XPS measurements provided further evidence for the MCE and AFM observations. The XPS spectra of the pristine PMMA show typical O 1s and C 1s peaks at 531 and 283, respectively (Figure 2B). On the QEAK16-II and EAK16-II-coated PMMA surfaces, N 1s signals appeared, which exists only in the amine groups of peptides and confirms the existence of peptide assemblies on the surface. However, the N 1s signal of QEAK16-II is about one-tenth of that obtained for EAK16-II. Based on the N 1s signal, the coverage of QEAK16-II is estimated as less than 10% on the PMMA surface (Table S1, see Supporting Information). The 81.0 ± 0.5° WCA of QEAK16-II was similar to the 81.7 ± 0.5° WCA of the pristine PMMA, whereas an obviously decreased WCA of 75.6 ± 1.9° was observed on the EAK16-II-coated PMMA (Table S2). XPS and WCA measurement further confirmed AFM observation that EAK16-II with free ε-NH_2 groups self-organized into a compact coating layer tightly adsorbed on the surface, whereas QEAK16-II with ε-$N(CH_3)_3$ groups formed barely adsorbed assemblies on the surface, suggesting the key role of ionic hydrogen bonding rather than electrostatic interaction in the self-assembly of peptides on the PMMA surface.

We then utilized ATR-FTIR spectroscopy to investigate the secondary structure of EAK16-II and QEAK16-II assemblies on the PMMA surface. The amide I band at 1600−1700 cm^{-1} largely due to the C═O stretching vibration of the peptide amide band has been widely used for studying secondary peptide structures.[42−46] The pristine PMMA and QEAK16-II-modified PMMA shows similar FTIR spectra with typical C═O stretching vibrations at 1729 cm^{-1} and no evident peaks due to the amide I band at 1600−1700 cm^{-1}. On the contrary, characteristic peaks attributed to α-helixes and β-sheets were clearly observed at 1656 and 1628 cm^{-1}, respectively, on the EAK16-II-coated PMMA surfaces (Figure 3A). These results

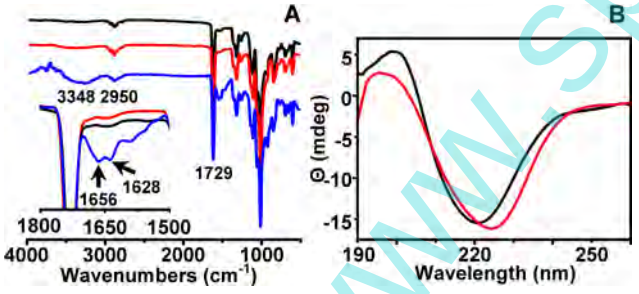

Figure 3. (A) ATR-FTIR spectra of the pristine PMMA (black line) as well as QEAK16-II-coated (red line) and EAK16-II-coated PMMA (blue line) surface. (B) CD spectra of 1.0 mg/mL EAK16-II (black line) and 1.0 mg/mL QEAK16-II (red line) in 10 mM phosphate buffer (pH 7.4).

suggested that very small amounts of QEAK16-II adsorbed on the surface compared with that of EAK16-II, consistent with AFM, XPS, and WCA observations. Particularly, the quaternization of ε-NH_2 groups has shown very little effect on the conformation of peptides in solution (Figure 3B and Table S3, see Supporting Information) but remarkably affected the self-assembly of peptides on the PMMA surface, indicating that spontaneous adsorption of peptides from solution to the PMMA surface is largely governed by ionic hydrogen bonding between free ε-NH_2 groups and surface negative charges.

Characterization of Nonspecific Protein Adsorption and Blood Compatibility on QEAK16-II- and EAK16-II-Coated PMMA Channels. We further performed a protein-repelling assay using BSA and LYZ as model proteins to investigate the competitive adsorption between peptides and proteins, i.e., relative affinity to the PMMA surface.[21,23] First, the pristine as well as QEAK16-II- and EAK16-II-coated PMMA microchannels were filled with 1.0 mg/mL FITC-BSA and FITC-LYZ in 10 mM phosphate buffer (pH 7.4) and incubated at 37 °C for 1 h. Afterward, the protein solution was removed, and the channels were dried under vacuum at 25 °C. After washing with copious DI water and drying under vacuum at 25 °C, the resulting protein contaminated microchannels were imaged by fluorescence (FL) microscopy for quantifying nonspecific protein adsorption. At a pH 7.4, BSA (pI 4.7) and LYZ (pI 11.0) are negatively and positively charged, respectively, and the PMMA surface is negatively charged. However, the fluorescence images show that both FITC-BSA and FITC-LYZ adsorbed strongly on the pristine and QEAK16-II-modified microchannels, whereas no significant adsorption was observed on the EAK16-II-coated microchannel (Figure S1, see Supporting Information). On the PMMA surface, QEAK16-II led to a 1.3% and 0.9% reduction in BSA and LYZ adsorption, respectively. Conversely, EAK16-II led to a 98.9% and 98.0% reduction in BSA and LYZ adsorption, respectively (Figure 4A). We also assessed platelet adhesion and thrombus

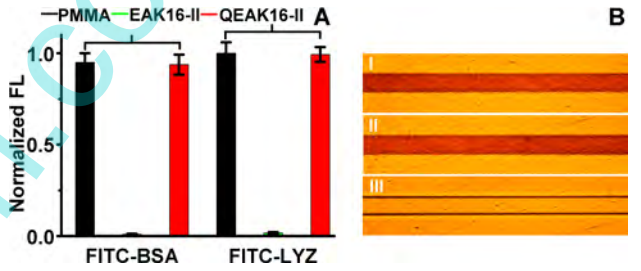

Figure 4. (A) Adsorption of FITC-BSA and FITC-LYZ on the PMMA microchannels, which correspond to the fluorescent micrographs in Figure S1. (B) Optical micrograph of the PMMA microchannels from whole blood flow tests. The pristine PMMA (I), QEAK16-II- (II), and EAK16-II-modified PMMA surface (III).

accumulation using whole blood flow testing.[22,23] As shown in Figure 4B and Figure S2, the whole blood, collected from a healthy person containing 3.8 wt % citrate sodium as anticoagulant, formed the coagulation and thrombus in the pristine and QEAK16-II-modified microchannels within 5 min (Figure 4BI and Figure S2I, Figure 4BII and Figure S2II). Inversely, EAK16-II-coated microchannel exhibited a clean channel without thrombus formation in 30 min (Figure 4BIII and Figure S2III). These results clearly demonstrated that EAK16-II with ionic hydrogen bonding readily self-organized into a complete and irreversible coating layer, which interacted with the surface via the same noncovalent forces as proteins. However, the tightly packed EAK16-II in the assemblies allowed more favorable intermolecular interactions including hydrogen bonding, hydrophobic, and van der Waals forces than proteins did. In general, the adsorption of EAK16-II on the surface is more energetically favorable than that of proteins. Therefore, EAK16-II has higher surface affinity than proteins and can not be replaced by standard proteins and concentrated complex proteins in blood, thus allowing excellent protein-repelling capacity and blood compatibility. In comparison, QEAK16-II without ionic hydrogen bonding formed assemblies with less than 10% coverage, which may easily be substituted by

DOI: 10.1021/acs.jpcc.6b05176
J. Phys. Chem. C 2016, 120, 19135−19141

proteins, thereby leading to serious nonspecific protein adsorption and extensive thrombosis very similar to those observed on the pristine PMMA surface.

Dynamic Coating of PMMA Microchannels Using EAK16-II, EAR16-II, and EAKR16-II for High-Performance Separation of Amino Acids, Peptides, and Proteins. Dynamic coating is a simple but vastly used surface modification method in electrophoresis applications,[23,26−29] in which coating additives in running buffers physically adsorbed on channel walls to form a coating layer for suppression of analytes adsorption. Based on the above results, if ionic hydrogen bonding plays a key role in adsorption of peptides and proteins on the PMMA surface, EAK16-II and its analogues with different basic amino acid residues in sequence such as EAR16-II and EAKR16-II will exhibit similar coating performance on the PMMA channels. As shown in Figure 5A, the

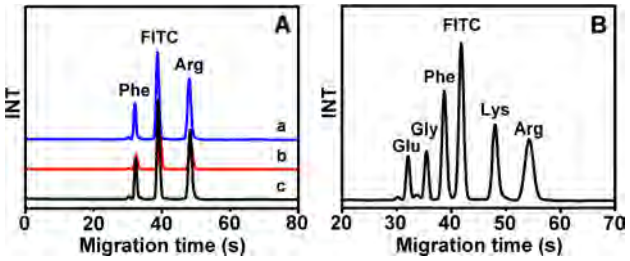

Figure 5. (A) Microchip electropherograms of FITC-labeled Phe and Arg (1.0×10^{-7} M) on the PMMA channels dynamically coated with 1.0 mg/mL EAKR16-II (a), EAR16-II (b), and EAK16-II (c). (B) Electropherogram of five FITC-labeled amino acids (1.0×10^{-7} M) on the PMMA microchannels dynamically coated with 1.0 mg/mL EAKR16-II. Conditions: 20 mM borate buffer, pH 9.4, E_{sep} = 270 V/cm, and the effective separation length of 30 mm.

highly reproducible separations of FITC-Phe and FITC-Arg were achieved on the PMMA microchannels dynamically coated with EAK16-II, EAR16-II, and EAKR16-II at the concentrations of 1.0 mg/mL or above in running buffers, and no evident differences in the separation efficiency and reproducibility were observed at buffer pH values between 8.0 and 11.0. The results clearly indicated that EAK16-II, EAR16-II, and EAKR16-II can self-organize into a complete coating layer on the PMMA channel and greatly suppress analyte adsorption, thus providing further evidence on the key role of ionic hydrogen bonding in the adsorption of peptides on the PMMA surface. The separation field strength from 200 to 410 V/cm and the buffer concentration from 10 to 50 mM were investigated with 1.0 mg/mL EAKR16-II dynamic coating, and the optimal ones were the separation field strength of 270 V/cm and the buffer concentration of 20 mM. Under the optimal conditions, the baseline separation of five FITC-labeled amino acids was achieved within 60 s with the theoretical plates of greater than 1.5×10^5 plates/m and the relative standard deviation (RSD) values of the migration times of less than 1.6% on four different PMMA microchannels (n = 4) (Figure 5B).

As shown in Figure 6A, FITC-labeled peptides, AE16-II and AR16-II, were well separated within 60 s in a 30 mm PMMA microchannel dynamically coated with 1.0 mg/mL EAKR16-II. The column efficiencies of 1.9×10^5 and 1.5×10^5 plates/m were obtained for FITC-AE16-II and FITC-AR16-II, respectively, which are almost the same as those for FITC-labeled amino acids, verifying the negligible nonspecific adsorption of peptides on the PMMA channel surface. Figure 6B shows the

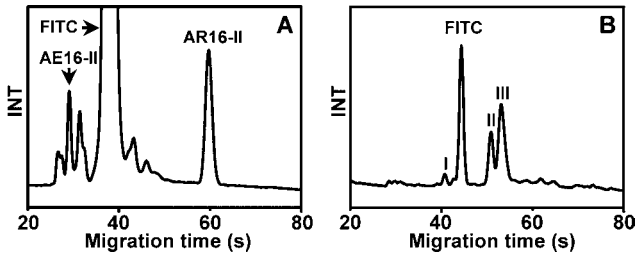

Figure 6. Microchip electropherograms of (A) FITC-labeled peptides and (B) FITC-labeled proteins on PMMA microchannels dynamically coated with 1.0 mg/mL EAKR16-II. I, β-latagobulin; II, ribonuclease A; III, chymptrypsinogen A. Conditions: 20 mM borate buffer, pH 9.4, E_{sep} = 270 V/cm, and the effective separation length of 30 mm.

separation of FITC-labeled β-latagobulin, ribonuclease A, and chymptrypsinogen A in a PMMA microchannel dynamically coated with 1.0 mg/mL EAKR16-II. The column efficiencies of 2.3×10^5, 1.9×10^5, and 1.6×10^5 plates/m were obtained for β-latagobulin, ribonuclease A, and chymptrypsinogen A, respectively, which are again at the same level as those for amino acids, indicating that the nonspecific adsorption of proteins was efficiently suppressed by the EAKR16-II dynamic coating. These results provided further evidence on the key role of the ionic hydrogen bonding between the free ε-NH_2 groups and the surface negative charges in strong adsorption of peptides and proteins on the PMMA surface.

4. CONCLUSIONS

In summary, self-assembly of ionic complementary peptides including EAK16-II, QEAK16-II, EAR16-II, and EAKR16-II on the PMMA surface was comprehensively studied using various techniques including MCE, AFM, ATR-FTIR, XPS, protein-repelling assay, and blood compatibility testing. We demonstrated the first sound evidence that the ionic hydrogen bonding between free lysine NεH and negative charges on the PMMA surface plays a key role in strong adsorption of peptides and proteins on the PMMA surface. Since most natural solid surfaces are negatively charged, the current research provides mechanistic insights into how peptides and proteins strongly interact with a solid surface at the molecular level, which opens up new possibilities for the future development of functionalized surfaces.

■ ASSOCIATED CONTENT

Supporting Information

The Supporting Information is available free of charge on the ACS Publications website at DOI: 10.1021/acs.jpcc.6b05176.

Tables S1−S3, Experimental Section, and Figures S1 and S2 (PDF)

■ AUTHOR INFORMATION

Corresponding Author

*E-mail dangfqn@snnu.edu.cn; Fax (+86) 29-8153-0727 (F.D.).

Author Contributions

N.L. and J.X. contributed equally to this work.

Notes

The authors declare no competing financial interest.

DOI: 10.1021/acs.jpcc.6b05176
J. Phys. Chem. C 2016, 120, 19135−19141

■ ACKNOWLEDGMENTS

This work was supported by the National Natural Science Foundation of China (No. 21175088).

■ REFERENCES

(1) Yeo, L. Y.; Chang, H. C.; Chan, P. P.; Friend, J. R. Microfluidic Devices for Bioapplications. *Small* **2011**, *7*, 12−48.
(2) Neužil, P.; Giselbrecht, S.; Länge, K.; Huang, T.; Manz, A. Revisiting Lab-on-a-Chip Technology for Drug Discovery. *Nat. Rev. Drug Discovery* **2012**, *11*, 620−632.
(3) Araci, I.; Su, B.; Quake, S.; Mandel, Y. An Implantable Microfluidic Device for Self-Monitoring of Intraocular Pressure. *Nat. Med.* **2014**, *20*, 1074−1078.
(4) Patabadige, D. E.; Jia, S.; Sibbitts, J.; Sadeghi, J.; Sellens, K.; Culbertson, C. T. Micro Total Analysis Systems: Fundamental Advancesand Applications. *Anal. Chem.* **2016**, *88*, 320−338.
(5) Tokel, O.; Inci, F.; Demirci, U. Advances in Plasmonic Technologies for Point of Care Applications. *Chem. Rev.* **2014**, *114*, 5728−5752.
(6) Chen, P.; Feng, X.; Sun, J.; Wang, Y.; Du, W.; Liu, B. Hydrodynamic Gating for Sample Introduction on a Microfluidic Chip. *Lab Chip* **2010**, *10*, 1472−1475.
(7) Siegel, A. C.; Tang, S. K.; Nijhuis, C. T.; Hashimoto, M.; Phillips, S.; Dickey, M. D.; Whitesides, G. M. Cofabrication: A Strategy for Building Multicomponent Microsystems. *Acc. Chem. Res.* **2010**, *43*, 518−528.
(8) Xu, Y.; Wang, C.; Li, L.; Matsumoto, N.; Jang, K.; Dong, Y.; Mawatari, K.; Suga, T.; Kitamori, T. Bonding of Glass Nanofluidic Chips at Room Temperature by a One-Step Surface Activation Using an O_2/CF_4 Plasma Treatment. *Lab Chip* **2013**, *13*, 1048−1052.
(9) Ren, K.; Zhou, J.; Wu, H. Materials for Microfluidic Chip Fabrication. *Acc. Chem. Res.* **2013**, *46*, 2396−2406.
(10) Kim, D.; Wu, X.; Young, A.; Haynes, C. Microfluidics-Based in Vivo Mimetic Systems for the Study of Cellular Biology. *Acc. Chem. Res.* **2014**, *47*, 1165−1173.
(11) Tran, N. T.; Ayed, I.; Pallandre, A.; Taverna, M. Recent Innovations in Protein Separationon Microchips by Electrophoretic Methods: An update. *Electrophoresis* **2010**, *31*, 147−173.
(12) Huh, D.; Matthews, B.; Mammoto, A.; Montoya-Zavala, M.; Hsin, H.; Ingber, D. Reconstituting Organ-Level Lung Functions on a Chip. *Science* **2010**, *328*, 1662−1668.
(13) Colace, T.; Tormoen, G.; McCarty, O.; Diamond, S. Microfluidics and Coagulation Biology Annual Review of Biomedical Engineering. *Annu. Rev. Biomed. Eng.* **2013**, *15*, 283−303.
(14) Chrimes, A.; Khoshmanesh, K.; Stoddart, P.; Mitchell, A.; Kalantarzadeh, K.; Microfluidics. and Raman Microscopy: Current Applications and Future Challenges. *Chem. Soc. Rev.* **2013**, *42*, 5880−5906.
(15) Wen, H.; Yu, Y.; Zhu, G.; Jiang, L.; Qin, J. A. Droplet Microchip with Substance Exchange Capability for the Developmental Study of C. elegans. *Lab Chip* **2015**, *15*, 1905−1911.
(16) Mu, X.; Zheng, W.; Sun, J.; Zhang, W.; Jiang, X. Microfluidics for Manipulating Cells. *Small* **2013**, *9*, 9−21.
(17) Culbertson, C. T.; Mickleburgh, T. G.; Stewart-James, S. A.; Sellens, K. A.; Pressnall, M. Micro Total Analysis Systems: Fundamental Advances and Biological Applications. *Anal. Chem.* **2014**, *86*, 95−118.
(18) Streets, A. M.; Zhang, X.; Cao, C.; Pang, Y.; Wu, X.; Xiong, L.; Yang, L.; Fu, Y.; Zhao, L.; Huang, Y.; et al. Microfluidic Single-Cell Whole-Transcriptome Sequencing. *Proc. Natl. Acad. Sci. U. S. A.* **2014**, *111*, 7048−7053.
(19) Kim, Y. T.; Lee, D.; Heo, H. Y.; Kim, D. H.; Seo, T. S. An Integrated Slidable and Valveless Microdevice with Solid Phase Extraction, Polymerase Chain Reaction, and Immunochromatographic Strip Parts for Multiplex Colorimetric Pathogen Detection. *Lab Chip* **2015**, *15*, 4148−4155.
(20) Zhuang, B.; Han, J.; Xiang, G.; Gan, W.; Wang, S.; Wang, D.; Wang, L.; Sun, J.; Li, C.; Liu, P. A Fully Integrated and Automated Micro System for Rapid Pharmacogenetic Typing of Multiple Warfarin-Related Single-Nucleotide Polymorphisms. *Lab Chip* **2016**, *16*, 86−95.
(21) Yang, L.; Li, L.; Tu, Q.; Ren, L.; Zhang, Y.; Wang, X.; Zhang, Z.; Liu, W.; Xin, L.; Wang, J. Photocatalyzed Surface Modification of Poly(dimethylsiloxane) with Polysaccharides and Assay of Their Protein Adsorption and Cytocompatibility. *Anal. Chem.* **2010**, *82*, 6430−6439.
(22) Zhang, Z.; Borenstein, J.; Guiney, L.; Miller, R.; Sukavaneshvar, S.; Loose, C. Polybetaine Modification of PDMS Microfluidic Devices to Resist Thrombus Formation in Whole Blood. *Lab Chip* **2013**, *13*, 1963−1968.
(23) Yu, X.; Xiao, J.; Dang, F. Surface Modification of Poly (dimethylsiloxane) Using Ionic Complementary Peptides to Minimize Nonspecific Protein Adsorption. *Langmuir* **2015**, *31*, 5891−5898.
(24) Bellanger, H.; Darmanin, T.; Givenchy, E. T.; Guittard, F. Chemical and Physical Pathways for the Preparation of Superoleophobic Surfaces and Related Wetting Theories. *Chem. Rev.* **2014**, *114*, 2694−2716.
(25) Dang, F.; Hasegawa, T.; Biju, V.; Ishikawa, M.; Kaji, N.; Yasui, T.; Baba, Y. Spontaneous Adsorption on a Hydrophobic Surface Governed by Hydrogen Bonding. *Langmuir* **2009**, *25*, 9296−9301.
(26) Dang, F.; Maeda, E.; Osafune, T.; Nakajima, K.; Kakehi, K.; Ishikawa, M.; Baba, Y. Carbohydrate Protein Interactions Investigated on Plastic Chips Statically Coated with Hydrophobically Modified Hydroxyethylcellulose. *Anal. Chem.* **2009**, *81*, 10055−10060.
(27) Prakash, S.; Karacor, M. B.; Banerjee, S. Surface Modification in Microsystems and Nanosystems. *Surf. Sci. Rep.* **2009**, *64*, 233−254.
(28) Zhou, J.; Khodakov, D. A.; Ellis, A. V.; Voelcker, N. H. Surface Modification for PDMS-Based Microfluidic Devices. *Electrophoresis* **2012**, *33*, 89−104.
(29) Peng, X.; Zhao, L.; Du, G.; Wei, X.; Guo, J.; Wang, X.; Guo, G.; Pu, Q. Charge Tunable Zwitterionic Polyampholyte Layers Formed in Cyclic Olefin Copolymer Microchannels through Photochemical Graft Polymerization. *ACS Appl. Mater. Interfaces* **2013**, *5*, 1017−1023.
(30) Wang, X.; Liu, G.; Zhang, G. Effect of Surface Wettability on Ion-Specific Protein Adsorption. *Langmuir* **2012**, *28*, 14642−14653.
(31) Puddu, V.; Perry, C. C. Peptide Adsorption on Silica Nanoparticles: Evidence of Hydrophobic Interactions. *ACS Nano* **2012**, *6*, 6356−6363.
(32) Jin, J.; Jiang, W.; Yin, J.; Ji, X.; Stagnaro, P. Plasma Proteins Adsorption Mechanismon Polyethylene-Grafted Poly(ethylene glycol) Surface by Quartz Crystal Microbalance with Dissipation. *Langmuir* **2013**, *29*, 6624−6633.
(33) Penna, M. J.; Biggs, M. J.; Mijajlovic, M. Molecular-Level Understanding of Protein Adsorption at the Interface between Water and a Strongly Interacting Uncharged Solid Surface. *J. Am. Chem. Soc.* **2014**, *136*, 5323−5331.
(34) Lehman, S. E.; Mudunkotuwa, I. A.; Grassian, V. H.; Larsen, S. C. Nano−Bio Interactions of Porous and Nonporous Silica Nanoparticles of Varied Surface Chemistry: A Structural, Kinetic, and Thermodynamic Study of Protein Adsorption from RPMI Culture Medium. *Langmuir* **2016**, *32*, 731−742.
(35) Fenoglio, I.; Fubini, B.; Ghibaudi, E. M.; Turci, F. Multiple Aspects of the Interaction of Biomacromolecules with Inorganic Surfaces. *Adv. Drug Delivery Rev.* **2011**, *63*, 1186−1209.
(36) Chen, H.; Yuan, L.; Song, W.; Wu, Z.; Li, D. Biocompatible Polymer Materials: Role of Protein−Surface Interactions. *Prog. Polym. Sci.* **2008**, *33*, 1059−1087.
(37) Kang, Y.; Li, X.; Tu, Y.; Wang, Q.; Ågren, H. On the Mechanism of Protein Adsorption onto Hydroxylated and Nonhydroxylated TiO_2 Surfaces. *J. Phys. Chem. C* **2010**, *114*, 14496−14502.
(38) Schwierz, N.; Horinek, D.; Liese, S.; Pirzer, T.; Balzer, B. N.; Hugel, T.; Netz, R. R. On the Relationship between Peptide Adsorption Resistance and Surface Contact Angle: A Combined Experimental and Simulation Single-Molecule Study. *J. Am. Chem. Soc.* **2012**, *134*, 19628−19638.
(39) Nagasawa, D.; Azuma, T.; Noguchi, H.; Uosaki, K.; Takai, M. Role of Interfacial Water in Protein Adsorption onto Polymer Brushes

DOI: 10.1021/acs.jpcc.6b05176
J. Phys. Chem. C 2016, 120, 19135−19141

as Studied by SFG Spectroscopy and QCM. *J. Phys. Chem. C* **2015**, *119*, 17193−17201.
(40) Meot-Ner, M. Update 1 of: Strong Ionic Hydrogen Bonds. *Chem. Rev.* **2012**, *112*, PR22−PR103.
(41) Sun, X.; Li, D.; Lee, M. Poly(ethylene glycol)-Functionalized Polymeric Microchips for Capillary Electrophoresis. *Anal. Chem.* **2009**, *81*, 6278−6284.
(42) Yang, H.; Pritzker, M.; Fung, S. Y.; Sheng, Y.; Wang, W.; Chen, P. Anion Effect on the Nanostructure of a Metal Ion Binding Self-Assembling Peptide. *Langmuir* **2006**, *22*, 8553−8562.
(43) Capes, J. S.; Kiley, P. J.; Windle, A. H. Investigating the Effect of pH on the Aggregation of Two Surfactant-Like Octapeptides. *Langmuir* **2010**, *26*, 5637−5644.
(44) Gelain, F.; Silva, D.; Caprini, A.; Taraballi, F.; Natalello, A.; Villa, O.; Nam, K. T.; Zuckermann, R. N.; Doglia, S. M.; Vescovi, A. BMHP1-Derived Self-Assembling Peptides: Hierarchically Assembled Structures with Self-Healing Propensity and Potential for Tissue Engineering Applications. *ACS Nano* **2011**, *5*, 1845−1859.
(45) Guilbaud, J. B.; Rochas, C.; Miller, A. F.; Saiani, A. Effect of Enzyme Concentration of the Morphology and Properties of Enzymatically Triggered Peptide Hydrogels. *Biomacromolecules* **2013**, *14*, 1403−1411.
(46) Lee, N. R.; Bowerman, C. J.; Nilsson, B. L. Effects of Varied Sequence Pattern on the Self-Assembly of Amphipathic Peptides. *Biomacromolecules* **2013**, *14*, 3267−3277.

DOI: 10.1021/acs.jpcc.6b05176
J. Phys. Chem. C 2016, 120, 19135−19141